Construction and Building Materials 315 (2022) 125766

Contents lists available at ScienceDirect

Construction and Building Materials

journal homepage: www.elsevier.com/locate/conbuildmat

Mechanical behavior of fiber reinforced slag-based geopolymer mortars incorporating artificial lightweight aggregate exposed to elevated temperatures

Sarah Kadhim [a], Abdulkadir Çevik [a], Anıl Niş [b,*], Derya Bakbak [c], Maysam Aljanabi [a]

[a] Department of Civil Engineering, Gaziantep University, Gaziantep, Turkey
[b] Department of Civil Engineering, Istanbul Gelisim University, İstanbul, Turkey
[c] The Grand National Assembly of Turkey, Ankara, Turkey

ARTICLE INFO

Keywords:
Lightweight geopolymer mortar
Artificial lightweight aggregate
PVA fibers
Mechanical properties
Elevated temperatures

ABSTRACT

The present research investigates the effects of artificial lightweight aggregate (ALWA) and polyvinyl alcohol (PVA) fiber utilization on the mechanical performance of slag-based lightweight geopolymer mortar (LGPM) specimens cured at ambient temperature. Also, the influence of elevated temperature (250 °C and 500 °C) on the resulting performance of LGPM samples was studied. For the production of LGPM specimens, 60% and 80% ALWA were utilized as a partial replacement of river sand. The slag-based LGPM samples were activated by a mixture of sodium silicate and 12 M sodium hydroxide solutions. The fresh and hardened state properties of LGPM specimens with and without fibers were assessed by workability, density, compressive strength, uniaxial tensile strength, and flexural strength tests. Also, the micro-scale variations were evaluated by scanning electron microscopy (SEM). The findings revealed that the incorporation of ALWA reduced the workability, density, and compressive strength of the LGPM, and the reductions in all these properties were more with 1% PVA inclusions. Meanwhile, inclusions of 1% PVA fibers significantly enhanced the uniaxial tensile and flexural behaviors of LGPM. After exposure to 250 °C, all mechanical strengths were improved due to the further geopolymerization, while mechanical strength reductions were observed at 500 °C due to the vapor impact and difference in thermal expansion. The uniaxial tensile strength of fiber-reinforced LGPM samples was improved from 1.47 MPa to 2.16 MPa at 250 °C, while uniaxial tensile strength reduced at 500 °C, and the samples exhibited a brittle failure mode due to the melting of PVA fibers. The results pointed out that tensile and flexural properties of LGPM significantly enhanced with ALWA and 1% PVA fiber utilization.

1. Introduction

One of the most significant issues facing the planet nowadays is environmental pollution. The generation rate of industrial and agricultural waste materials or by-products is growing vastly day by day. For example, around fifteen million tons of fly ash (FA) and more than 500,000 tons of ground granulated blast furnace slag (GGBS) are produced in Turkey every year [1]. With the environmental concerns associated with the disposal of these wastes to landfills properly, the reuse of such materials can be helpful to preserve the global environment [2]. To date, researchers focused on the partial use of cementitious materials (slag, fly ash, silica fume etc.) in concrete production to reduce environmental concerns [3]. Also, significant research has been conducted on the application of nanomaterials and innovative materials to improve mechanical performance and durability of cement-based materials [4–11]. The concrete industry can offer a solution for waste management and depleting natural resources such as natural sand or cement by using waste and by-product materials as alternatives to cement or aggregate, without affecting the quality of the final product. Geopolymer is a promising alternative binder to concrete, an eco-friendly and environmentally friendly construction material. Geopolymers have shown excellent mechanical and durability characteristics with lower production costs and lower greenhouse gas emissions than traditional cement binders [12]. As far as the properties of the geopolymers were concerned, the advantages of using them are many, for example, reduced creep and shrinkage, superior chemical attack

* Corresponding author at: Department of Civil Engineering, Istanbul Gelisim University, İstanbul, Turkey.
E-mail address: anis@gelisim.edu.tr (A. Niş).

https://doi.org/10.1016/j.conbuildmat.2021.125766
Received 27 August 2021; Received in revised form 16 November 2021; Accepted 17 November 2021
Available online 26 November 2021
0950-0618/

Table 1
Chemical composition and physical properties of GGBS.

CaO	SiO_2	Al_2O_3	Fe_2O_3	MgO	SO_3	K_2O	Na_2O	Specific gravity	Blaine fineness (m^2/kg)	Loss on ignition
34.12%	36.4%	10.39%	0.69%	10.3%	0.49%	0.97%	0.35%	2.79	418	1.64

resistance, improved strength, lower porosity, and earlier development of strength than OPC as they gain 70% of their final strength in the first few hours of curing [13]. Furthermore, compared with traditional cement-based materials, geopolymers have low heat conductivity and great resistance to fires even if they are exposed to 1200C because of their characteristics which are similar to ceramics [14].

Numerous studies have been conducted on the production and the possibility of using geopolymers in the construction industry. Geopolymer is formed via the alkali activation of aluminosilicate materials, such as metakaolin, FA, or GGBS, at elevated or ambient temperatures to manufacture a polymeric base gel [15]. Different studies have indicated that GGBS has superior properties, making it a promising material to accelerate the reaction of the alkaline binder. GGBS can be used as a sole material in forming geopolymer, and it is more reactive with self-cementing characteristics due to its high content of calcium oxides [16]. Generally, it was reported that the utilization of GGBS improved the strength, microstructure, and durability of geopolymers [17]. A study by Li and Liu [18] found that 70 MPa compressive strength at 14 days had been achieved from using 4% GGBS in geopolymer mortar specimens.

From the viewpoint of decreasing the use of natural aggregates and increasing the utilization of waste materials in generating construction materials, the creation and use of artificial aggregates is an effective solution for producing a sustainable aggregate with reduced energy consumption. The utilization of FA in the manufacturing of artificial aggregates seemed to be a promising way to solve waste management. The FA lightweight aggregates can be produced using three techniques: sintering, autoclaving or cold bonding. Among these methods, the cold bonding process is the most economical method since it requires a minimum amount of energy to produce the aggregate [19]. Mermerdas et al. [13] used FA to produce artificial lightweight aggregate (ALWA) through the cold bonded method. The research findings stated that using ALWA with a 100% replacement level improved the geopolymer mortar workability. However, they concluded that increasing ALWA content in mortar samples adversely influenced the compressive strength, resulting from the poor and soft structure. Abdulkareem et al. [20] studied the effects of high temperatures on the properties of geopolymer mortars containing ALWA. They observed that the low thermal conductivity of the lightweight aggregates improved the properties of the mortars and enhanced their fire resistance.

Many researches have been realized in the last decades on fibrous concrete. The inclusion of fibers in the concrete mix is an effective way to improve the mechanical characteristics of concrete, for instance, enhancing its toughness, ductility, flexural, tensile, and cracking distribution control [21]. It is better to mention that different fiber types/scales (e.g., nanofibers and nanotubes) have been investigated [22–26]. Since nanofibers/tubes cannot improve the post-peak behavior due to the small length (typically below 30 μm), this study investigates the effect of microfibers; particularly PVA fibers in this research. Several researches stated that adding polyvinyl alcohol fibers (PVA) is an efficient method to enhance the fresh properties, such as the workability, and the hardened properties, such as ductility and toughness, which have a favorable influence on reducing cracks propagation, thus raising the fracture toughness of geopolymers [27]. For instance, Arisoy and Wu [28] produced PVA fiber-reinforced lightweight concrete. The study's findings revealed an improved flexural strength with an excellent toughness compared with the non-fibrous lightweight concrete samples. Tanyildizi and Yonar [29] performed an investigation on the influences of high temperature on the mechanical performance of PVA fiber-reinforced fly ash-based geopolymer concrete. The results revealed that the compressive and flexural strengths of the geopolymer concrete improved with an increase in the PVA fiber content. In another investigation of Li and Du [30], they developed PVA fiber-reinforced geopolymer mortar using fly ash. They reported that PVA fibers improved the flexural toughness by bridging the cracks.

There is a very limited study regarding the utilization of PVA fibers in lightweight artificial aggregate incorporating geopolymer mortars. Thus, this research focused on the effectiveness of using PVA fibers by examining the mechanical properties, such as compressive, flexural, and uniaxial tensile strengths. In addition, the influence of elevated temperature on the LWGM samples was also investigated.

2. Experimental study

2.1. Materials

In the research, ground granulated blast furnace slag (GGBS) was used to produce lightweight geopolymer mortars. Table 1 shows the chemical and physical properties of GGBS. Natural river sand, which is locally available, was used with a particle size in the range of 0 to 4 mm, a fineness modulus of 2.86, a specific gravity of 2.68, and water absorption of 0.58%. The artificial fly ash aggregates developed by the cold bonding process were utilized to manufacture LWGM specimens. These artificial aggregates were developed in the construction laboratory using a pelletizer disc to agglomerate 90 percent of fly ash with 10 percent of cement, as shown in Fig. 1. The aggregate fresh pellets were produced after 20 min. Then, the pellets were coated with plastic sheets and left for curing in the laboratory for 28 days at room temperature. At the end

Fig. 1. ALWA manufacturing process [1]

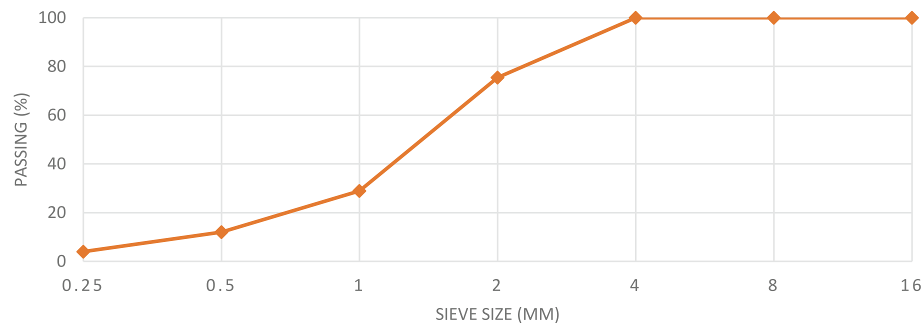

Fig. 2. ALWA grading curve.

Table 2
Properties of PVA fibers

Diameter (μm)	Length (mm)	l/d ratio	Young's modulus (GPa)	Elongation (%)	Nominal strength (MPa)	Density (g/ cm^3)
39	12	308	41	6	1600	1.3

Table 3
Mix proportions of LGPM mixes.

Mix ID	GGBS	Activators NaOH solution	Na_2SiO_3 solution	Aggregates Natural	Artificial	SP	Extra water	PVA fiber(%)
60%A-0%F	500	114.3	285.7	600	900	15	20	0
80%A-0%F	500	114.3	285.7	300	1200	25	50	0
80%A-1%F	500	114.3	285.7	300	1200	75	50	1.0

Note: All values are in kg/ m^3 , except for fiber content, which is a volume fraction.

of the curing process, the produced pellets were sieved to separate 0.25–4 mm fine particles. The detailed artificial lightweight aggregate (ALWA) production was given in the previous study [1]. The produced artificial aggregates have a fineness modulus of 2.79 and a specific gravity of 1.76 g/ cm^3 . Their gradation curve is shown in Fig. 2.

The sodium hydroxide and sodium silicate mixture was utilized as the alkali activator. The chemical composition of the used sodium silicate solution consists of 55.5% water, 29.7% silicon dioxide, and 14.7% sodium oxide (by mass). Master Glenium RMC 303, a high range water-reducing admixture, was utilized in all mixes to achieve the required workability. In addition, the polyvinyl alcohol (PVA) fibers were incorporated in some mixtures with a fiber fraction of 1% by volume to study the influence of PVA fibers on the resulting performance of LWGM samples. Table 2 indicates the properties of the used PVA fibers in this study.

2.2. Mixing, casting, and curing

Three slag-based lightweight geopolymer mortar (LGPM) mixtures were prepared in the study; two mixtures without fibers and one with PVA fibers. These mixes were denoted as 60%A-0%F, 80%A-0%F, and 80%A-1%F. The designation of LGPM mixes was based on the investigated parameters; the A indicated the replacement level of the lightweight artificial aggregate (60%A and 80%A), and the F pointed out the PVA fiber volume fraction (0%F and 1%F). Thus, for example, 80%A-1% F indicates the replacement level of fine aggregate by artificial aggregate

Fig. 3. Geopolymer mortars stored in plastic bags.

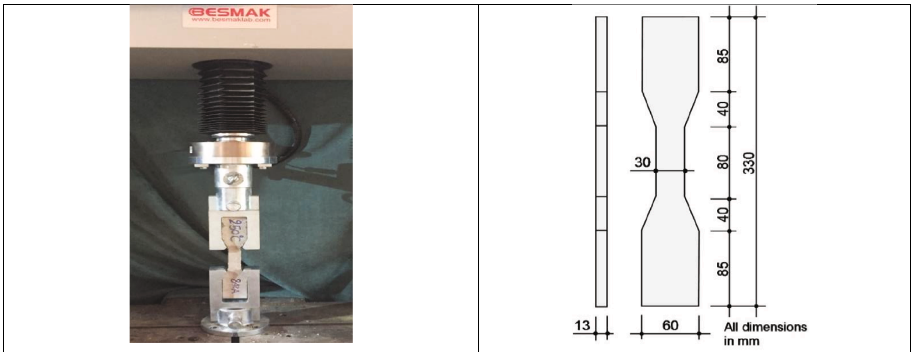

a) sample under uniaxial tensile strength test | b) sample dimensions [34]

Fig. 4. Uniaxial tensile strength test setup.

is 80%, and the volume fraction of PVA fibers is 1%. Several LGPM trial batches were cast and tested, and the mixes which achieved the best cohesive and workable LPGM were selected as shown in Table 3 for detailed analyses.

The NaOH flakes were dissolved in water, and then the solution was stored at an ambient temperature to cool before being used. All through the study, the concentration of NaOH was kept constant at 12 M, which was performed superior mechanical and durability performance [31]. After that, 12 M NaOH solution and Na_2SiO_3 solution were mixed together with a sodium silicate to hydroxide ratio of 2.5. The obtained alkaline solutions were then left in plastic containers at ambient temperature for at least 24 h to allow heat dissipation before utilization. All mixes were composed based on a constant binder (GGBS) amount and alkaline activator solution, where the activator to binder ratio was 0.8. The proportion of binder to aggregate ratio was 1:3. These values were chosen after doing some trial mixes to attain the desired strength with acceptable workability. According to previous research, the volume ratio of PVA fibers ranged between 0.2% and 2% [27]. In the present experimental work, the PVA fiber volume fraction was selected as 1% for economy.

The mixing process started by mixing the dry ingredients (i.e., GGBS, river sand, and ALWA) for 3 min. Then, the alkali activator solution was gradually added to the dry materials and mixed for 4 min. After the water and superplasticizer were slowly added to the mixer, the mixing was continued for 5 min. to obtain proper workability. For the workability enhancement and further geopolymerization, additional water is also utilized in the mixes [32]. It should be noted that the water to geopolymer solids ratio by mass is significant in designing geopolymer samples. Additional water dilutes the liquids, which causes a reduction in mechanical strengths. Therefore, additional water usage for the workability improvement should be limited in geopolymer mixes to prevent mechanical strength reduction. For the fibrous mixes, the PVA fibers were slowly included in the mixer to satisfy uniform fiber dispersion and the mixture continued at high speed for 3 min. After the mixing period was finished, the obtained fresh mix was cast into different pre-oiled molds in two layers and well-compacted using a table vibrator to remove the air voids. Then, all the molds were coated by a thin plastic film to minimize the alkali activator solution loss and left in the laboratory for 24 h. The samples were then demolded and stored in plastic bags, as shown in Fig. 3. Ambient curing was adopted in this research since it was reported that slag-based geopolymer concretes can be used in structural elements without elevated temperature or water curing [32].

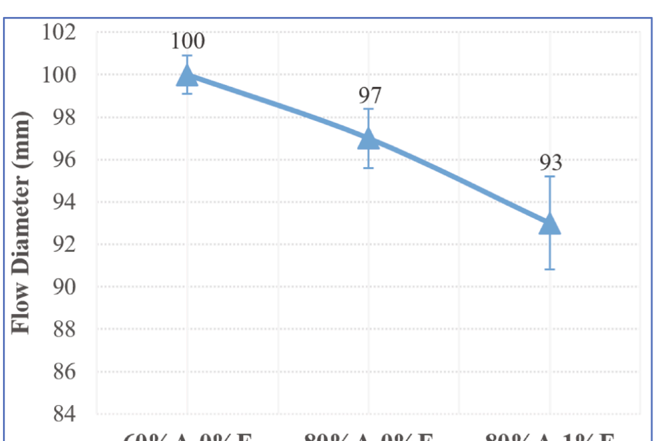

Fig. 5. Flows of LGPM mixes.

2.3. Test procedure

The workability of lightweight geopolymer mortar mixtures was defined by a flow table test. The test was conducted on each mortar mix according to ASTM C1437 [33]. The fresh density of each geopolymer mortar mix was determined as soon as the mixing process was finished. Meanwhile, the hardened density was measured just before the compressive strength tests. For the hardened state tests, compressive strength tests were executed using three 70 mm side cubes, and the average compressive strength was calculated by taking the average of the three companion specimens. Also, cylinder specimens of 100 mm in diameter and 200 mm in height were utilized for compressive strength tests, conducted under displacement-controlled loading at a 0.5 mm/min rate using a universal testing machine. Load and displacement data were obtained for each cylinder sample. Before performing the test, the sulfur capping procedure was carried out to level the surfaces of each sample.

The flexural tests were executed on the prism and beam samples with dimensions of 160 mm × 40 mm × 40 mm and 350 mm × 75 mm × 45 mm, respectively, after 28 days of curing. The flexural response of the LGPM specimens was investigated by the three-point bending tests under a constant loading rate of 0.3 mm/min until the specimens failed. To measure displacements at the midpoint of the span of the samples, linear variable displacement transducers were utilized. The load vs. displacement data were recorded and plotted.

The uniaxial tensile behavior of LGPM samples was evaluated through the tensile test. The test setup and dimensions of the dog-bone samples are presented in Fig. 4. The shape of the dog-bone specimens causes the majority of cracks to happen in the narrow section of 80 mm in the middle of the specimen. The specimens were subjected to quasi-static uniaxial tension loadings up to the failure. The tensile stress vs. strain curves were plotted throughout the tests.

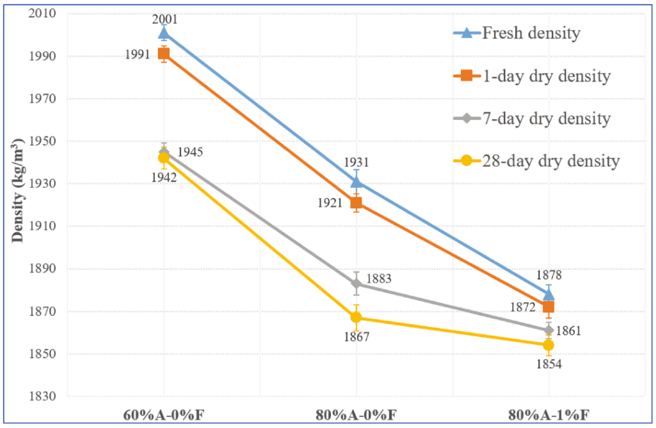

Fig. 6. Fresh and dry densities of LGPM mixes.

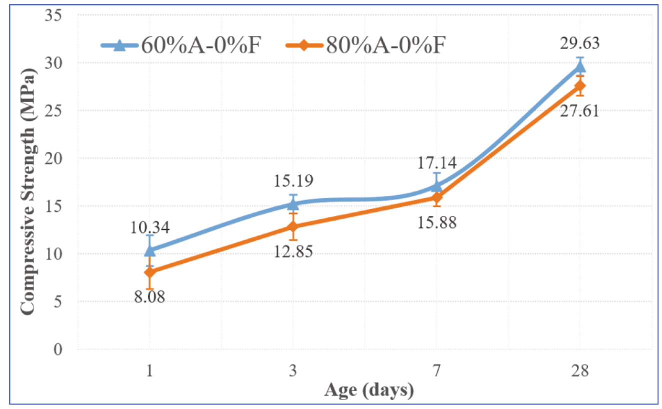

Fig. 7. Compressive strength of geopolymer mortars at different substitution levels of ALWA.

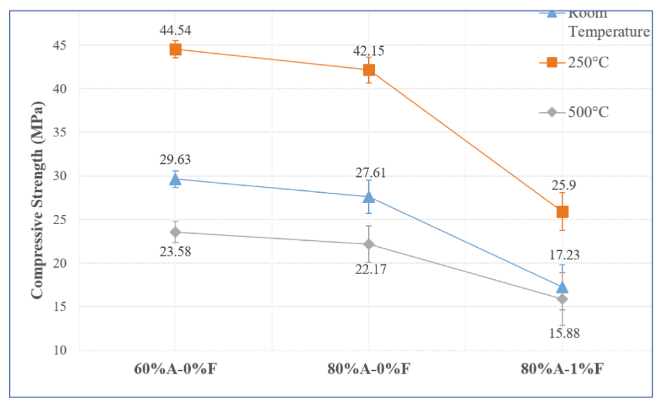

Fig. 8. Variations of compressive strength of LGPM at different exposure temperatures.

2.4. Exposure to elevated temperatures

A series of samples were exposed to temperatures of 250 °C and 500 °C to analyze the impact of high temperature on the behavior of lightweight geopolymer mortar samples (with and without PVA fibers). The specimens were put in an oven and heated at a heating rate of 25 °C/min until the target temperature was reached. The samples were then kept at each elevated temperature for 30 min. Then, the samples were allowed to cool inside the oven to room temperature without subjecting them to thermal shock. For comparative purposes, the properties of lightweight mortar samples were tested before and after exposure to the elevated temperature.

3. Test results and discussion

3.1. Flow Table test

Fig. 5 shows the workability of different geopolymer mortar mixtures. The findings revealed that the flowability reduced slightly with an increase in the replacement level of artificial lightweight aggregate (ALWA). It can be attributed to dry surface condition of ALWA particles, adsorbing a higher amount of liquid and reducing the workability. Also, the incorporation of PVA fibers had further decreased the workability due to the large surface area of PVA fibers, resulting in increased adherence between the mortar and the aggregates. A similar result was stated in the previous investigation [35]. Meanwhile, it is worth mentioning that there was no segregation or bleeding in the LGPM mixes with/out fibers. In general, the artificial lightweight aggregates with rounded particles have a low ability to form bleeding [17].

3.2. Density test

Fig. 6 presents the measured densities (fresh and dry) at various curing ages based on the different replacements of river sand by ALWA for the non-reinforced and reinforced geopolymer mortars. It was observed that the densities of geopolymer mixes decreased by increasing the volume replacement of river sand by ALWA due to the moisture condition and the lower density of ALWA. Furthermore, a gradual reduction in the density of the LGPM mixtures was obtained by increasing the age of samples from 1 day to 28 days. This reduction can be attributed to water evaporation and the development of the geopolymer matrix [36].

In fiber-reinforced LGPM specimens, the inclusion of PVA fibers to LGPM decreased both the fresh and the dry densities. The fresh density was found 2.7% lower than that of the mix without fibers (80%A-0%F). However, the variation of dry density was not significant (0.7% lower than that of the 80%A-0%F mix). This can be attributed to the low specific gravity of PVA fibers, resulting in a reduction in the density of LGPM samples. Moreover, the porosity of the LGPM specimens became higher due to the fiber inclusions [15]. Overall, according to ACI Committee 213R-03 [37], the upper limit of density to consider air-dried mortars as lightweight mortars is defined as 1950 kg/ m^3 . As there is no specification for geopolymer mortars, this criterion can also be applied for geopolymer mortars. The results showed that the dry densities of all LGPM mixtures are less than 1950 kg/ m^3 , which can be considered lightweight.

3.3. Compressive strength performance

3.3.1. Compressive strength of cube specimens

Fig. 7 illustrates the average compressive strengths at 1 day, 3 days, 7 days, and 28 days of geopolymer mortars prepared with variable replacement levels of ALWA. The findings showed that the compressive strength increased with the curing age due to the continuous geopolymerization process. Also, increasing the substitution level of ALWA from 60% to 80% reduced the compressive strength by 21.9%, 15.4%, 7.4%, and 6.8% at 1 day, 3 days, 7 days, and 28 days, respectively. The reason for the reduction is that lightweight aggregates are usually weaker than river sand particles due to their porous nature. Moreover, the smooth surface of ALWA, compared with river sand with a rough surface, decreased the adherence to the geopolymer matrix, which would be another cause of the strength reduction. Besides, increasing the substitution level of river sand by ALWA reduced the density, as mentioned previously. As a result, the compressive strengths reduced. These results are in agreement with the findings of previous

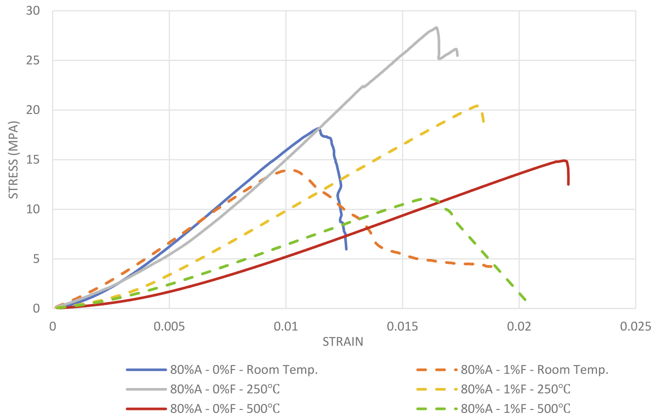

Fig. 9. Stress vs. strain curves of LGPM cylinders under compression at elevated temperatures.

investigations [13,38]. Generally, according to ACI Committee 213 [37], the compressive strengths of all specimens were in the range of 17 MPa and 41.0 MPa, which can be utilized as lightweight structural concrete in structural applications.

The compressive strength of the geopolymer specimens incorporating PVA fibers (80%A-1%F) was found 37.6% lower than that of the specimens without PVA fibers at 28 days, as shown in Fig. 8. In literature, the reduction in compressive strength was reported when PVA fiber incorporations exceeded 0.8% [21], attributed to the more air content and voids in LGPM specimens [39]. It is noted that the LGPM specimens containing PVA fibers showed good resistance to crack propagation due to the bridging mechanism of the PVA fibers. After compressive strength tests, the specimens with PVA fibers showed no separation and high resistance to LGPM brittle failure. Also, the specimen maintained its original shape after peak load, resulting in a ductile failure mode [40].

Fig. 8 also demonstrates the influences of elevated temperatures (250C and 500C) on the compressive strengths of LGPM specimens. The results revealed an increase in the compressive strengths for all LGPM specimens at 250C compared with the specimens at room temperature.

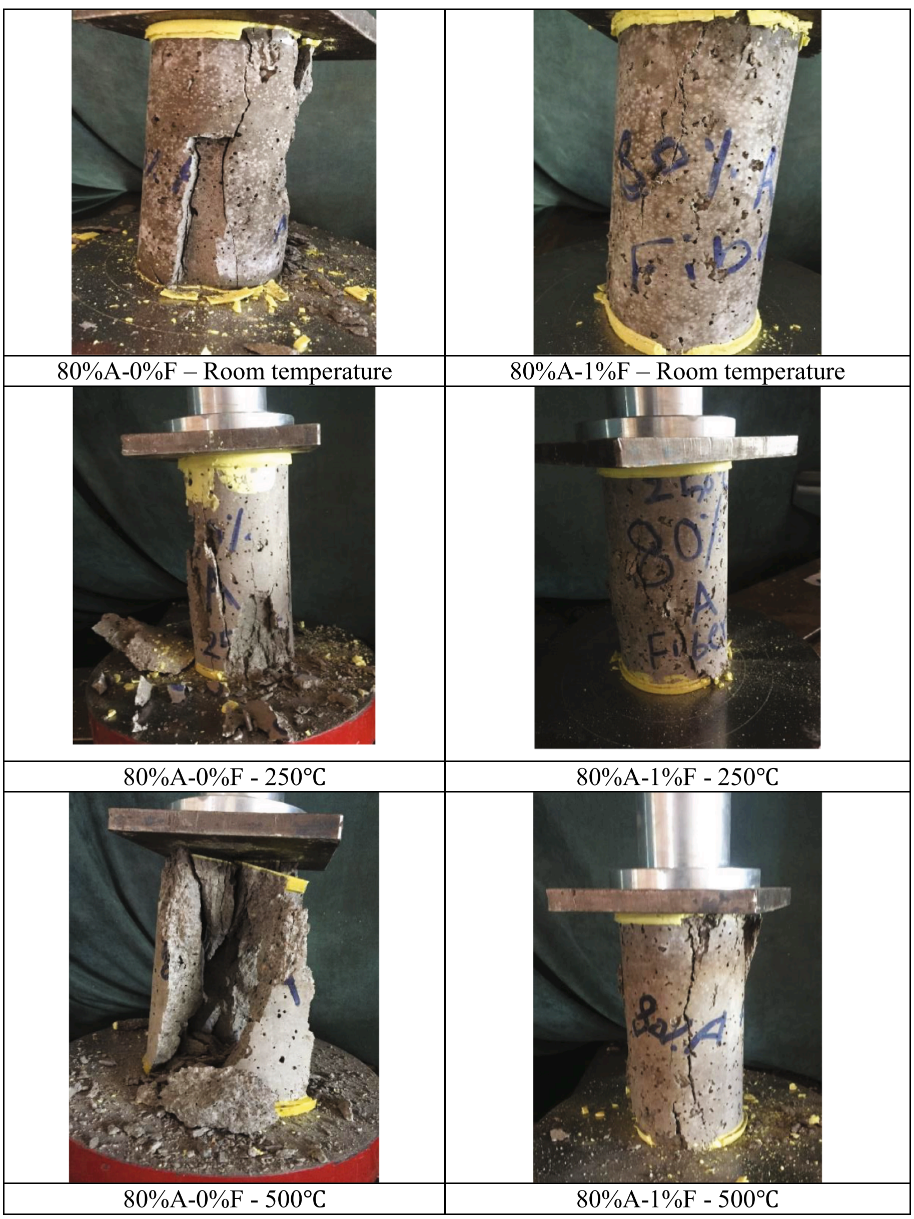

Fig. 10. Failure modes of LGPM cylinder samples after compressive test.

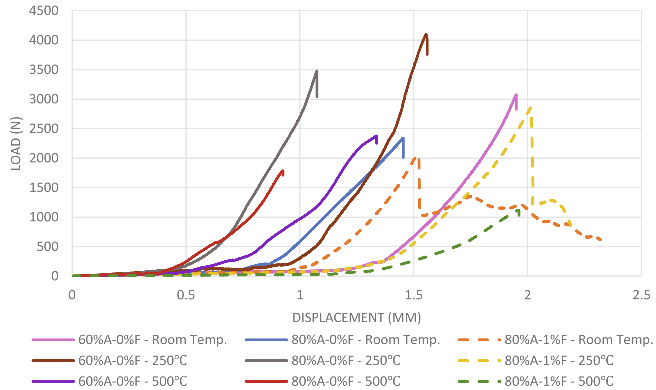

Fig. 11. Load-displacement curves of LGPM prism specimens at various temperatures.

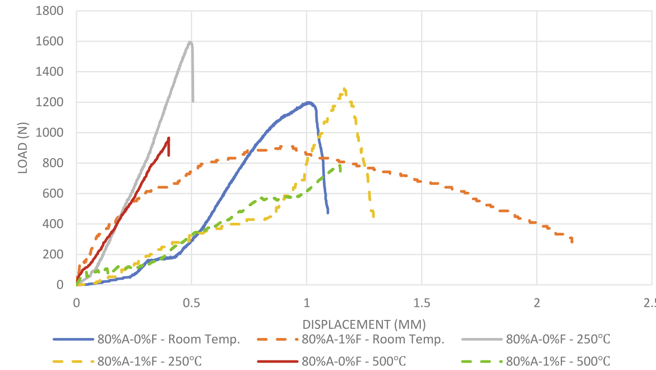

Fig. 12. Load-displacement curves of LGPM beam specimens at various temperatures.

The compressive strength increase at 250C may be attributed to the internal autoclaving process and filling up of the pores with extra CSH and CASH formation, leading to a more compact structure with low porosity and high mechanical performance [41,42]. Furthermore, the denser structure of binding paste can be related to the accelerated geopolymerization reactions between alkaline solution and GGBS at elevated temperatures [43].

However, after the exposure to 500C , the LGPM specimens exhibited a reduction in the compressive strengths due to a large number of microcracks developing at 500 °C. At this temperature, the compressive strength reductions compared with the samples at room temperature were 20.4%, 19.7%, and 7.8% for 60%A-0%F, 80%A-0%F, and 80%A-1%F, respectively. A similar finding was reported in the previous research [44]. The strength reduction at 500 °C can be attributed to the high thermal shrinkage due to the water vaporization from geopolymers. The free water turns to water vapor at 500 °C, rising vapor pressure. When the vapor pressure comes to its absolute limit, the matrix with low permeability cannot withstand the high thermal stresses, causing thermal cracks on the surface, leading to a reduction of compressive strength.

3.3.2. Stress–strain relationship of cylinder specimens

Fig. 9 depicts the stress–strain curves of cylinder specimens of LGPM under compression at different temperatures. Generally, the curves consist of three stages; elastic deformation stage, plastic deformation stage, and falling stage, which occurs after reaching the peak load. The findings revealed a 23% reduction in the compressive strength due to adding PVA fibers. However, in terms of the compressive strain, it can be seen that the specimen with 1% PVA fibers has a greater strain. Fiber-reinforced samples can demonstrate the ability to deform and maintain a high load level even after reaching the peak load, displaying a state of steady cracking. Moreover, there was no sudden and brittle failure observed in the specimens reinforced with PVA fibers, which may be attributed to the crack-bridging capacity of PVA fibers, as stated in the earlier investigation [45].

Fig. 9 also shows the stress vs. strain curves for LGPM specimens at elevated temperatures. At 250 °C, the compressive strength increased due to the progressive geopolymerization process and water evaporation, leading to an increment in Van der Walls force [46]. Moreover, the specimens with PVA fibers exhibited higher strain levels compared with the non-reinforced specimens. Incorporating PVA fibers improved the cracking response by resisting the expansion and forming confinement in the circumferential direction.

However, there was a slight decrease in the compressive strengths when the temperature reached up to 500 °C. The compressive strength reductions were 17.9% and 20.4% for 80%A-0%F and 80%A-1%F, respectively. This reduction can be attributed to micro-crack development, possible phase-change transition in geopolymers, and differential thermal expansion between geopolymer matrix and PVA fibers. Additionally, as the temperature was increased, the compressive strains of specimens also increased, resulting from a significant change in material behavior [47]. By comparing all of the curves, it can be discovered that the samples exposed to 500 °C exhibited the highest strains. As revealed in Fig. 10, the samples without PVA fibers suffered severe spalling and cracking, while the LGPM samples containing PVA fibers suffered minor damage. PVA fibers resisting the cracks and hold specimens in a one-piece at room temperature and 250 °C. However, after exposure to 500 °C, spalling occurred due to the melting of PVA fibers at higher temperatures (greater than250–300 °C)

3.4. Flexural behavior

Figs. 11 and 12 demonstrate the load–displacement curves of LGPM prism and beam specimens (with and without fibers) at elevated temperatures, respectively. The results revealed that increasing the replacement level of artificial lightweight aggregates (ALWA) decreased the displacement and the load-carrying capacity by about 26% and 24%, respectively. The reason for this could be that increasing ALWA content increased the brittleness and damage of LGPM specimens due to the softness of ALWA particles. The load–displacement curves of ALWA incorporated samples showed a linear upward slope and then a load drop after reaching the peak load in correspondence to the formation of the cracks inside the specimen until failure.

With the incorporation of PVA fibers, there is an increase in the displacements compared to the non-reinforced specimens, as shown in Figs. 11 and 12. For instance, adding PVA fibers in prismatic specimens exhibited 60% more displacement capacity for the displacement of plain samples, Fig. 11. This phenomenon could be attributed to the crack bridging of the PVA fibers. The strain-softening behavior was observed for the PVA fiber-reinforced prismatic samples, while a brittle behavior was noticed for the samples without fibers. In Fig. 12, the fiber-reinforced beam specimens showed a strain hardening behavior after the first cracking. This could be due to the formation and propagation of cracks inside the specimen. After the peak load, a descending curve was obtained in the specimens until failure. Incorporating PVA fibers improved the ductility and toughness of LGPM specimens, and failure types became more ductile, which was significant, especially in high seismic zones. The visual observations throughout the flexural test revealed that for the non-fibrous LGPM, the cracking began in the mid-span and rapidly spread to the top. Then the specimens were broken into two halves at ultimate load, indicating a brittle failure mode. On the other hand, the fibrous LGPM specimens demonstrated ductility and continued to carry the load after the first crack and delayed the failure of the specimens.

The load-carrying capacity was increased for the specimens exposed to 250 °C. This increase was higher for the plain (80%A-0%F) prism specimens than for the beam specimens by 48.6% and 33.1%,

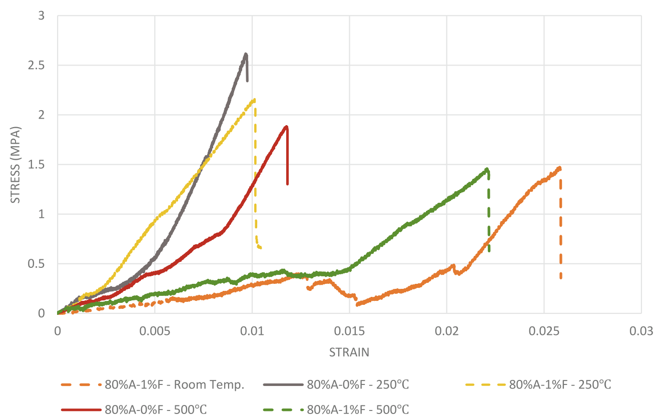

Fig. 13. Tensile stress vs. strain curves of dog-bone samples at elevated temperatures.

respectively, compared to those of the unheated specimens. However, it was observed that the displacement values were lower for all LGPM samples exposed to elevated temperatures than the unexposed specimens. The reduction in ductility was observed at 250 °C. On the other hand, the displacement capacity of the PVA-reinforced specimens was still greater than the non-fibrous samples, which may be attributed to the heat transfer of fibers throughout the specimens, reducing the localized thermal damage in the matrix. However, the ductility of specimens decreased compared to room temperature, indicating that melting of some PVA fibers occurred during an elevated temperature of 250 °C, resulting in a reduction of ductility.

For the specimens exposed to 500 °C, the load-carrying capacity and displacements were declined for all LGPM mixtures. The reduction was found greater on the prism specimens than the beam specimens due to the size effect. As the size of the specimens increased, the degradation of specimens due to elevated temperature on the flexural behavior became more [48]. At 500 °C, most of the PVA fibers burned and became viscous and shrank, thereby remained fibers lost their ability to bridge the cracks. In addition, the higher temperatures reduced the elastic modulus of the fibers and the chemical bond between the fibers and the LGPM matrix. At 500 °C, the prism specimens exhibited a brittle failure while the beam specimens showed a strain-softening behavior with some ductility. At elevated temperatures, the ductility was reduced, and this reduction could be related to the number of cracks formed in the samples [34].

3.5. Uniaxial tensile performance

Fig. 13 illustrates the uniaxial tensile stress vs. strain behaviors of the different LGPM dog-bone specimens after exposure to 250C and 500C . LGPM specimens reinforced with PVA fibers after exposure to 250C showed a significant improvement in tensile strength from 1.47 MPa to 2.16 MPa due to the further geopolymerization. However, the tensile strain capacity reduced significantly, and the PVA fiber-reinforced LGPM specimens exhibited a brittle failure. It had been reported that the melting point of PVA fibers is about 225C [49], so this could be the reason for the reduction in the tensile strain capacity. However, the remaining PVA fibers were still able to participate in bridging the specimen, Fig. 14. Meanwhile, the non-fibrous LGPM specimen showed the highest tensile strength of 2.6 MPa and the lowest tensile strain capacity (6.6% lower than the reinforced specimen). Therefore, the non-fibrous specimen showed a brittle failure mode, Fig. 13.

With increasing the temperature from 250C to 500C , the tensile strengths of LGPM samples decreased to 1.9 MPa and 1.6 MPa for the samples without and with PVA fibers, respectively. This reduction in strength occurred due to thermal incompatibility, resulting in damage to the specimen [50]. However, tensile strain capacities increased by increasing the temperature for both reinforced and unreinforced samples to 2.2% and 1.2%, respectively, compared to those at 250C . The deterioration of LGPM tension stiffness had induced this due to varying degrees of thermal decomposition [49].

The tensile strain capacity is proportional to the number of cracks on the surface of the sample. Therefore, the strain capacity increased as the number of fine cracks increased [49]. It had been observed that multiple micro-cracks were formed during the loading of the fiber-reinforced samples, and most of them were closed after the unloading. In general, the failure of the samples occurred within the gauge length of the dog-bone samples (approximately within the middle portion, Fig. 14).

3.6. Scanning electron microscopy (SEM)

Fig. 15 shows the SEM micrographs of the LGPM specimens with/out PVA fibers before and after exposure to elevated temperatures. Fig. 15.a and 15.d show that increasing the replacement level of river sand by ALWA increased the number of broken particles on the failure surface. This can be attributed to the low stiffness of ALWA particles, resulting in

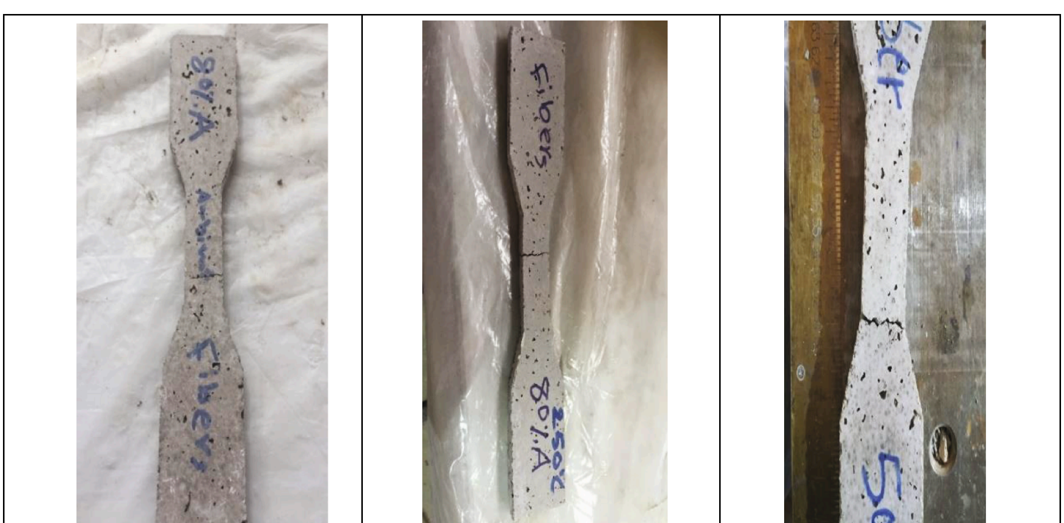

(a) at room temperature | (b) after exposure to 250°C | (c) after exposure to 500°C

Fig. 14. Failure crack patterns of 80%A-1%F dog-bone specimens under uniaxial tensile load.

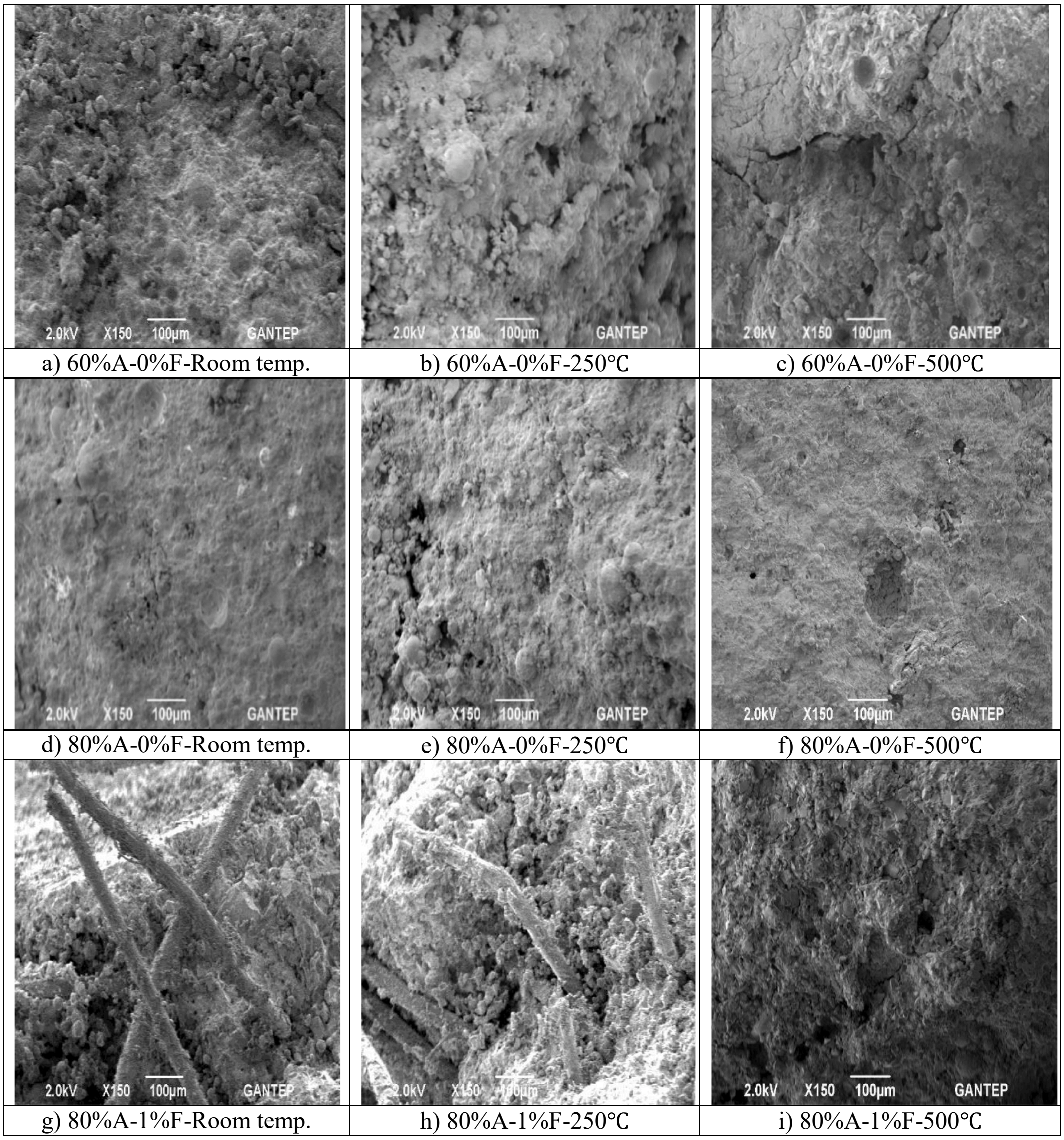

Fig. 15. SEM images of LGPM before and after exposure to elevated temperatures.

a decrease in the compressive strength results. Also, from these figures, there are some geopolymeric gel regions surrounded by the geopolymeric mortar, indicating incomplete geopolymeric reactions. Fig. 15. b and 15.e present the SEM micrographs of LGPM samples after exposure to 250C . It can be noticed that there was not a big difference in the microstructure appearance of LGPM at ambient temperature. However, some voids and micropores were detected due to water evaporation. Furthermore, SEM micrographs of the samples exposed to 500C exhibit a higher degree of degradation in the microstructure where micro-cracks and more voids had been formed, as shown in Fig. 15.c and 15.f. The significant loss of water in LGPM, and the variation in thermal expansion between ALWA and geopolymer paste during heating, could cause this deterioration, which is also correlated with the loss in compressive strengths, as shown in Fig. 8.

Meanwhile, microstructural analyses of PVA fibers at elevated temperatures were also conducted, as shown in Fig. 15.g – 15.i. As shown from Fig. 15.g, there is good adhesion between the fibers and the matrix. The fibers were coated by geopolymerization products formed during the geopolymerization reaction process, improving the bond between the fibers and the matrix [16]. Fig. 15.h illustrates the SEM micrographs of the specimens at 250C . The findings revealed that the fiber surfaces did not change significantly, and the geopolymer matrix still coated the surfaces. However, the SEM micrographs of the fibers after exposure to 500C showed that micro-channels emerged due to the melting of PVA fibers at this temperature, as shown in Fig. 15.i. These melted fibers increased the matrix porosity and resulted in the loss of mechanical performance and ductility. The pore pressure inside the LGPM samples was reduced due to the formation of these channels, enabling the escape of water vapor to the outside, reducing the likelihood of spalling.

4. Conclusions

The main findings of the experimental study could be summarized as follows:

- Considering the flow table test results, it can be concluded that increasing ALWA content in geopolymer mortar mixes reduced the flow diameter. Also, PVA fibrous mortars exhibited lower workability compared to non-fibrous mortars.
- Both fresh and dry density values were reduced by increasing the ALWA content due to the low density of ALWA. Density values of PVA fibrous LGPM samples were further reduced due to the low specific gravity of PVA fibers. The dry density of all the mixes was lower than 1950 kg/ m^3 , satisfying the specifications for lightweight

concrete structures, which is significant, especially in high seismic zones in the Marmara region, Turkey.

- The compressive strengths of LGPM showed that the strengths increased with age. The increase of ALWA content from 60% to 80% reduced the strength values by 6.8% at 28 days. Also, the inclusion of PVA fibers led to a reduction in the compressive strengths.
- After exposure to elevated temperatures, the compressive strength of LGPM samples increased at 250℃. However, the compressive strength values were decreased at 500C due to the degradation of specimens.
- From the stress–strain curves of cylindrical LGPM samples, incorporating PVA fibers reduced the compressive strength while increased the compressive strain. In addition, the compressive strength increased due to the ongoing geopolymerization process at 250 °C. However, compressive strength and ductility reductions were observed at 500 °C.
- Flexural behavior results revealed that increasing the ALWA content led to a reduction in both the displacement and the load-carrying capacity. However, the mortar mixes with PVA fibers showed higher displacements compared to the specimens without fibers. The PVA fibers remarkably improve the flexural characteristics of LGPM samples and change failure modes from brittle to ductile.
- After exposure to 250 °C, there was an increase in the flexural load-carrying capacity while a reduction in displacement capacity. However, a reduction in both flexural load-carrying capacity and displacement capacity was obtained at 500 °C.
- The uniaxial tensile strength results indicated that the uniaxial tensile strength of fibrous mortar samples was significantly improved from 1.47 MPa to 2.16 MPa at 250 °C, while a decrease in the tensile strain capacity was observed. At 500℃, the uniaxial tensile strength was reduced, while the tensile strain capacities were increased, and the samples exhibited a brittle failure mode.

Geopolymers have the potential to replace traditional cement and become an essential element of a sustainable construction sector. In summary, the current study showed that it is possible to produce LGPM using ALWA and PVA fibers with significantly improved mechanical properties at ambient curing, making LGPM suitable for in situ applications. For future study, other durability performances, i.e., chemical durability, should be thoroughly investigated for the standardization process.

CRediT authorship contribution statement

Sarah Kadhim: Investigation, Data curation, Writing – original draft. **Abdulkadir Çevik:** Conceptualization, Methodology, Supervision, Project administration, Resources. **Anıl Niş:** Conceptualization, Methodology, Visualization, Writing – original draft, Writing – review & editing. **Derya Bakbak:** Conceptualization, Methodology, Resources. **Maysam Aljanabi:** Investigation, Data curation, Writing – original draft.

Declaration of Competing Interest

The authors declare that they have no known competing financial interests or personal relationships that could have appeared to influence the work reported in this paper.

References

[1] J.M. Their, M. Özakça, Developing geopolymer concrete by using cold-bonded fly ash aggregate, nano-silica, and steel fiber, Constr. Build. Mater. 180 (2018) 12–22.
[2] S.H. Sanni, R.B. Khadiranaikar, Performance of alkaline solutions on grades of geopolymer concrete, International Journal of Research in Engineering and Technology 2 (11) (2013) 366–371.
[3] F. Dabbaghi, A. Sadeghi-Nik, N.A. Libre, S. Nasrollahpour, Characterizing fiber reinforced concrete incorporating zeolite and metakaolin as natural pozzolans, Structures 34 (2021) 2617–2627.
[4] A. Bahari, A. Sadeghi-Nik, F.U.A. Shaikh, A. Sadeghi-Nik, E. Cerro-Prada, E. Mirshafiei, M. Roodbari, Experimental studies on rheological, mechanical, and microstructure properties of self-compacting concrete containing perovskite nanomaterial, Structural Concrete (2021), https://doi.org/10.1002/suco.202000548.
[5] M.H. Khalilpasha, A. Sadeghi-Nik, O. Lotfi-Omran, K. Kimiaeifard, M. Amirpour-Molla, July). Sustainable development using recyclable rubber in self-compacting concrete, in: In Third international conference on construction in developing countries (advancing civil, architectural and construction engineering & management), 2012, pp. 580–585.
[6] A. Sadeghi-Nik, A. Bahari, Z. Khorshidi, R. Gholipur, July). Effect of lanthanum oxide on the bases of cement and concrete, in: In Third international conference on construction in developing countries (Advancing Civil, Architectural and Construction Engineering & Management), 2012, pp. 4–6.
[7] A. Bahari, A. Sadeghi-Nik, E. Cerro-Prada, A. Sadeghi-Nik, M. Roodbari, Y. Zhuge, One-step random-walk process of nanoparticles in cement-based materials基于一步随机游走法预测纳米颗粒在水泥基材料中的迁移, Journal of Central South University 28 (6) (2021) 1679–1691.
[8] S.M. MOSAVI, A. SADEGHI NIK, Strengthening of steel–concrete composite girders using carbon fibre reinforced polymer (CFRP) plates, Sadhana 40 (1) (2015) 249–261.
[9] A. Bahari, A. Sadeghi Nik, M. Roodbari, K. Taghavi, S.E. Mirshafiei, SYNTHESIS AND STRENGTH STUDY OF CEMENT MORTARS CONTAINING SiC NANO PARTICLES, Digest Journal of Nanomaterials & Biostructures (DJNB) 7 (4) (2012) 1427–1435.
[10] A. Bahari, A. Sadeghi-Nik, M. Roodbari, A. Sadeghi-Nik, E. Mirshafiei, Experimental and theoretical studies of ordinary Portland cement composites contains nano LSCO perovskite with Fokker-Planck and chemical reaction equations, Constr. Build. Mater. 163 (2018) 247–255.
[11] A.S. Nik, A. Bahari, Nano-particles in concrete and cement mixtures, In Applied Mechanics and Materials 110 (2012) 3853–3855.
[12] P. Zhang, Y. Zheng, K. Wang, J. Zhang, A review on properties of fresh and hardened geopolymer mortar, Compos. B Eng. 152 (2018) 79–95.
[13] Mermerdas, K., Süleyman, İ. P. E. K., SOR, N. H., MULAPEER, E. S., & EKMEN, Ş. (2020). The Impact of Artificial Lightweight Aggregate on the Engineering Features of Geopolymer Mortar. *Türk Doğa ve Fen Dergisi*, *9*(1), 79-90.
[14] S. Mane, H.S. Jadhav, Investigation of geopolymer mortar and concrete under high temperature, Magnesium 1 (5) (2012) 384–390.
[15] B. Nematollahi, J. Sanjayan, F.U. Ahmed Shaikh, Tensile Strain Hardening Behavior of PVA Fiber-Reinforced Engineered Geopolymer Composite, J. Mater. Civ. Eng. 27 (10) (2015) 04015001, https://doi.org/10.1061/(ASCE)MT.1943-5533.0001242.
[16] Y. Ling, K. Wang, W. Li, G. Shi, P. Lu, Effect of slag on the mechanical properties and bond strength of fly ash-based engineered geopolymer composites, Compos. B Eng. 164 (2019) 747–757.
[17] L.A.T. Bui, C.L. Hwang, C.T. Chen, M.Y. Hsieh, Characteristics of cold-bonded lightweight aggregate produced with different mineral admixtures Vol. 174 (2012) 978–983.
[18] Z. Li, S. Liu, Influence of slag as additive on compressive strength of fly ash-based geopolymer, J. Mater. Civ. Eng. 19 (6) (2007) 470–474.
[19] E. Güneyisi, M. Gesoğlu, Özgür Pürsünlü, K. Mermerdaş, Durability aspect of concretes composed of cold bonded and sintered fly ash lightweight aggregates, Compos. B Eng. 53 (2013) 258–266.
[20] O.A. Abdulkareem, A.M. Al Bakri, H. Kamarudin, I.K. Nizar, Ala'eddin, A. S., Effects of elevated temperatures on the thermal behavior and mechanical performance of fly ash geopolymer paste, mortar and lightweight concrete, Constr. Build. Mater. 50 (2014) 377–387.
[21] A. Niş, N. Özyurt, T. Özturan, Variation of Flexural Performance Parameters Depending on Specimen Size and Fiber Properties, J. Mater. Civ. Eng. 32 (4) (2020) 04020054, https://doi.org/10.1061/(ASCE)MT.1943-5533.0003105.
[22] M. Ramezani, Y.H. Kim, Z. Sun, Elastic modulus formulation of cementitious materials incorporating carbon nanotubes: Probabilistic approach, Constr. Build. Mater. 274 (2021) 122092, https://doi.org/10.1016/j.conbuildmat.2020.122092.
[23] M.A. Mousavi, A. Sadeghi-Nik, A. Bahari, C. Jin, R. Ahmed, T. Ozbakkaloglu, J. de Brito, Strength optimization of cementitious composites reinforced by carbon nanotubes and titania nanoparticles, Constr. Build. Mater. 303 (2021) 124510, https://doi.org/10.1016/j.conbuildmat.2021.124510.
[24] M. Ramezani, Y.H. Kim, Z. Sun, Mechanical properties of carbon-nanotube-reinforced cementitious materials: database and statistical analysis, Mag. Concr. Res. 72 (20) (2020) 1047–1071.
[25] M. Ramezani, Y.H. Kim, Z. Sun, Modeling the mechanical properties of cementitious materials containing CNTs, Cem. Concr. Compos. 104 (2019) 103347, https://doi.org/10.1016/j.cemconcomp.2019.103347.
[26] M. Ramezani, Y.H. Kim, Z. Sun, Probabilistic model for flexural strength of carbon nanotube reinforced cement-based materials, Compos. Struct. 253 (2020) 112748, https://doi.org/10.1016/j.compstruct.2020.112748.
[27] P. Zhang, K. Wang, J. Wang, J. Guo, S. Hu, Y. Ling, Mechanical properties and prediction of fracture parameters of geopolymer/alkali-activated mortar modified with PVA fiber and nano-SiO2, Ceram. Int. 46 (12) (2020) 20027–20037.
[28] B. Arisoy, H.-C. Wu, Material characteristics of high performance lightweight concrete reinforced with PVA, Constr. Build. Mater. 22 (4) (2008) 635–645.

[29] H. Tanyildizi, Y. Yonar, Mechanical properties of geopolymer concrete containing polyvinyl alcohol fiber exposed to high temperature, Constr. Build. Mater. 126 (2016) 381–387.

[30] W. Li, H. Du, in: April). Properties of PVA fiber reinforced geopolymer mortar, Springer, Cham, 2018, pp. 557–564.

[31] R. Alzeebaree, A.O. Mawlod, A. Mohammedameen, A. Niş, Using of recycled clay brick/fine soil to produce sodium hydroxide alkali activated mortars, Adv. Struct. Eng. 24 (13) (2021) 2996–3009.

[32] A. Niş, İ. Altındal, Compressive Strength Performance of Alkali Activated Concretes under Different Curing Conditions, Periodica Polytechnica Civil Engineering 65 (2) (2021) 556–565.

[33] ASTM, C1437–07, Standard Test Method for Flow of Hydraulic Cement Mortar, ASTM International, West Conshohocken, Pennsylvania, United States, 2007.

[34] S. Pourfalah, Behaviour of engineered cementitious composites and hybrid engineered cementitious composites at high temperatures, Constr. Build. Mater. 158 (January) (2018) 921–937.

[35] A.C. Bhogayata, N.K. Arora, Utilization of metalized plastic waste of food packaging articles in geopolymer concrete, J. Mater. Cycles Waste Manage. 21 (4) (2019) 1014–1026.

[36] Şevin Ekmen, K. Mermerdaş, Z. Algın, Effect of oxide composition and ingredient proportions on the rheological and mechanical properties of geopolymer mortar incorporating pumice aggregate, Journal of Building Engineering 34 (2021) 101893, https://doi.org/10.1016/j.jobe.2020.101893.

[37] ACI Committee 213. (2003). Guide for structural lightweight-aggregate concrete. *American Concrete Institute. Manual of Concrete Practice. Farmington Hills, Michigan, USA*.

[38] B. Nematollahi, R. Ranade, J. Sanjayan, S. Ramakrishnan, Thermal and mechanical properties of sustainable lightweight strain hardening geopolymer composites, Archives of Civil and Mechanical Engineering 17 (1) (2017) 55–64.

[39] Q. Frayyeh, A. Swaif, T.S. Al-Attar, M.A. Al-Neami, W.S. AbdulSahib, Mechanical properties of fly ash geopolymer mortar reinforced with carbon fibers, MATEC Web of Conferences 162 (2018) 02028, https://doi.org/10.1051/matecconf/201816202028.

[40] S. Xu, M.A. Malik, Z. Qi, B. Huang, Q. Li, M. Sarkar, Influence of the PVA fibers and SiO2 NPs on the structural properties of fly ash based sustainable geopolymer, Constr. Build. Mater. 164 (2018) 238–245.

[41] S.M.A. El-Gamal, F.I. El-Hosiny, M.S. Amin, D.G. Sayed, Ceramic waste as an efficient material for enhancing the fire resistance and mechanical properties of hardened Portland cement pastes, Constr. Build. Mater. 154 (2017) 1062–1078.

[42] F.A. Selim, M.S. Amin, M. Ramadan, M.M. Hazem, Effect of elevated temperature and cooling regimes on the compressive strength, microstructure and radiation attenuation of fly ash–cement composites modified with miscellaneous nanoparticles, Constr. Build. Mater. 258 (2020) 119648, https://doi.org/10.1016/j.conbuildmat.2020.119648.

[43] Şinasi Bingöl, C. Bilim, C.D. Atiş, Uğur Durak, Durability Properties of Geopolymer Mortars Containing Slag, Iranian Journal of Science and Technology - Transactions of Civil Engineering 44 (S1) (2020) 561–569.

[44] A. Wongsa, V. Sata, B. Nematollahi, J. Sanjayan, P. Chindaprasirt, Mechanical and thermal properties of lightweight geopolymer mortar incorporating crumb rubber, J. Cleaner Prod. 195 (2018) 1069–1080.

[45] L. Kan, L. Zhang, Y. Zhao, M. Wu, Properties of polyvinyl alcohol fiber reinforced fly ash based Engineered Geopolymer Composites with zeolite replacement, Constr. Build. Mater. 231 (2020) 117161, https://doi.org/10.1016/j.conbuildmat.2019.117161.

[46] Nayel, I. H., Nasr, M. S., & Abdulridha, S. Q. (2020). Impact of elevated temperature on the mechanical properties of cement mortar reinforced with rope waste fibres. In *IOP Conference Series: Materials Science and Engineering* (Vol. 671, No. 1, p. 012080). IOP Publishing.

[47] P. Behera, V. Baheti, J. Militky, S. Naeem, Microstructure and mechanical properties of carbon microfiber reinforced geopolymers at elevated temperatures, Constr. Build. Mater. 160 (2018) 733–743.

[48] K.N. Abdulhaleem, M.E. Gülşan, A. Çevik, Mechanical behavior of steel fiber-reinforced self-compacting concrete corbels after exposure to elevated temperatures, Structural Concrete 19 (6) (2018) 1881–1894.

[49] J.-C. Liu, K.H. Tan, Fire resistance of strain hardening cementitious composite with hybrid PVA and steel fibers, Constr. Build. Mater. 135 (2017) 600–611.

[50] Z. Pan, J.G. Sanjayan, B.V. Rangan, An investigation of the mechanisms for strength gain or loss of geopolymer mortar after exposure to elevated temperature, J. Mater. Sci. 44 (7) (2009) 1873–1880.